ISSN 0391-2612

ofioliti

VOLUME 19 • N. 2a • DECEMBER 1994 • PP. 177 - 330

An International Journal
on Ophiolites and Related Topics

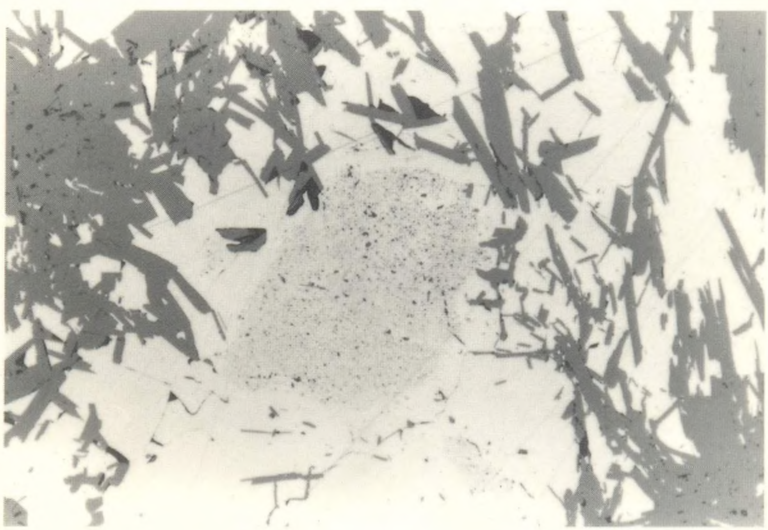

PITAGORA EDITRICE BOLOGNA

Ofioliti 1994, 19 (2a), 257-268

MINERAL ASSEMBLAGES OF THE GANKUVAYAM OPHIOLITIC SECTION IN THE KUYUL OPHIOLITIC TERRANE OF THE RUSSIA FAR EAST

Alexander I. Khanchuk and **Ivan V. Panchenko**
Far East Geological Institute, Vladivostok, Russia.

Keywords: *ophiolite, petrography, mineralogy, Kuyul terrane, Gankuvayam section.*

Abstract

We report a geochemical study of minerals occurring in the Gankuvayam ophiolitic section, belonging to the Kuyul ophiolitic terrane (Middle Triassic-Jurassic). The studied rocks include mantle harzburgite, cumulus gabbro-wehrlite, plagiogranite, basalt-ferroandesite-dacite sheeted dike, and pillow lavas. This rock complex forms a sequence bearing some specific features of a magmatic assemblage erupted in a supra-subduction zone. Upsection, regular variations of the mineral chemistry consistent with variations in lithology are apparent. Pyroxenes provide estimates of temperature, which shows decreasing values from harzburgite to gabbro-wehrlite to gabbro. Phase compositions particularly of spinel, give consistent indications that magmas were generated in a supra-subduction zone setting.

INTRODUCTION

The Kuyul ophiolites crop out to the northwest of the Kamchatka Peninsula in the Talovskiye Mountains of the Penjinsky Ridge. Ophiolites make up an allochthonous unit 120 km long and 10-50 km wide, enclosed in an Early Cretaceous accretionary prism (Alekseev, 1981; Chekhov, 1982; Khanchuk et al., 1990) (Fig. 1). They consist of a serpentinite melange, which includes blocks of harzburgite, gabbro, sheeted dikes, and basalts associated with pelagic sedimentary rocks. Middle Triassic and Norian-Early Jurassic cherts are interbedded with limestones, and Norian-Rhaetian and Late Jurassic cherts are found among the sedimentary rocks (Khanchuk et al., 1990).

The Late Jurassic Gankuvayam ophiolitic section lies within the Kuyul Terrane (61°44' Lat. North and 165°8' Long. East) and consists of a sequence of harzburgite, gabbro-troctolite-wehrlite, plagiogranite, sheeted dike, and pillow lavas. Dikes are aligned across the trend of the Kuyul Massif. Judging from the regular pattern of the chilled zones, the Gankuvayam thrust sheet is an ancient spreading center, preserving major features of oceanic hydrothermal metamorphism and hydrothermal sulphide mineralization (Khanchuk et al., 1990). This paper is devoted to the characteristics of the primary mineral associations of the ophiolite section.

PETROGRAPHY

The Gankuvayam ophiolite thrust sheet forms the core of a synform (Fig. 2), the limbs of which consist of serpentinized harzburgite and zones of serpentinite melange. Fig. 3 shows the complete cross-section of the Gankuvayam ophiolite sheet consisting of the following rock units (upwards): harzburgite (thickness: 420 m), dunite (50 m), layered gabbro, wehrlite and massive gabbro

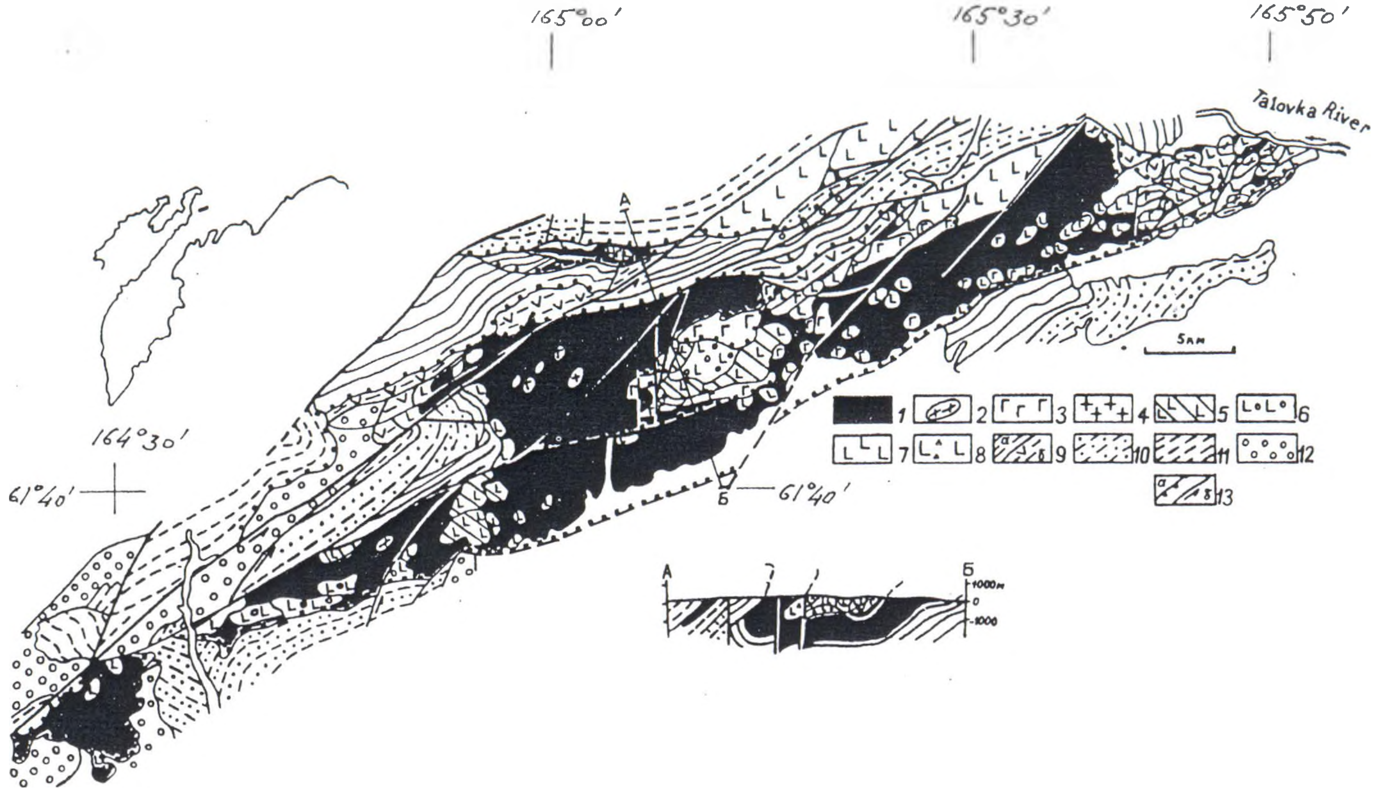

Fig. 1 - Geological sketch of the Kuyul ophiolitic terrane. After Khanchuk et al. (1990).

1-11 - accretionary wedge rocks: 1 - harzburgites and serpentinite melange; 2 - blocks of schists and amphibolites in the serpentinite melange; 3 - gabbros; 4 - plagiogranite; 5 - sheeted dikes; 6 - pillow-lavas and Triassic-Jurassic sedimentary rocks; 7 - dikes and pillow-lavas (not separated); 8 - breccias; 9 - Berriasian-Valanginian turbidites; 10 - Hauterivian-Barremian turbidites and olistostrome; 11 - Aptian-Albian turbidites; 12 - post-accretionary, Late Cretaceous and Paleogene clastic rocks; 13 - thrusts (a) strike-slip faults (b). A-B - Gankuvayam cross-section.

(340 m), plagiogranite (40 m), sheeted dikes (400 m) and pillow lavas (300).

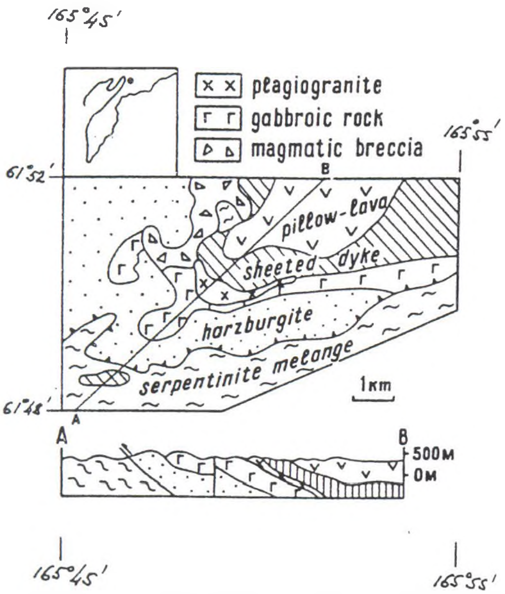

Fig. 2 - Geological scheme of the Gankuvayam ophiolitic section.

Harzburgite complex. Serpentinized harzburgite predominates in the ultramafic part of the section. Strongly serpentinized dunites were observed near the gabbroic rocks. On the basis of chemical composition some clinopyroxene-bearing rocks could be attributed to lherzolite. No typical lherzolite with low-chromian spinel was found. Primary minerals of the harzburgite are olivine (70-80% of the rock), orthopyroxene (20-30%), clinopyroxene (0-5%), and chromian spinel (1-2%). Orthopyroxene, clinopyroxene, and chromian spinel form anhedral crystals occurring among the olivine grains. The alternation of olivine and orthopyroxene results in some banding. Dislocation metamorphism was observed, like flexural cleavage cracks and cloudy crystal extinction.

Gabbro-wehrlite complex. Gabbro, troctolite, and wehrlite are interlayered. The gabbros include gabbro, gabbronorite, olivine gabbro, and olivine gabbronorite. Olivine gabbro predominates at the base, and gabbronorite, commonly with olivine, in the upper part. Troctolite occurs in the middle of the gabbroic section. Troctolite consists of serpentinized olivine (40%), plagioclase (50%), and chromian spinel. Wehrlite consists of olivine (60 to 70%), clinopyroxene (20 to 30%), and chromian spinel. Scattered plagioclase and orthopyroxene were observed. Wehrlite beds vary in thickness from 0.5 to 15 m.

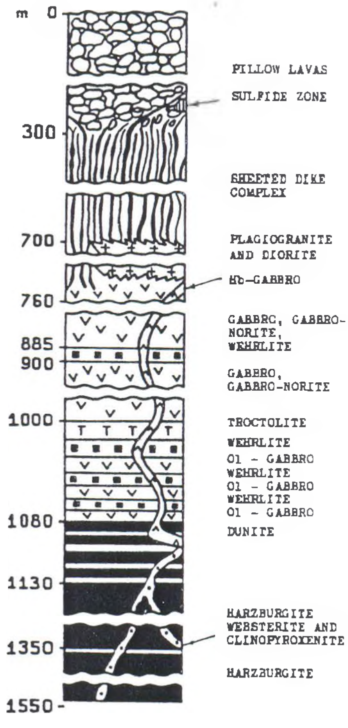

Fig. 3 - Stratigraphic column of the Gankuvayam section.

"Vein" series. Veins of coarse-grained websterite and clinopyroxenite occur in the ultramafic part of the section. Their thickness varies from 10-30 cm to several meters. In

the gabbroic section, veins are composed of fine-grained plagioclase-amphibole rocks.

The analysis of minerals from several samples of metasomatic veins shows that the clinopyroxene veins contain high chromian spinel and alumina spinel.

Plagiogranite complex. Plagiogranites form lenses of 40 to 60 cm thickness occurring between the gabbroic rocks and the dikes. Numerous inclusions of melanocratic rocks similar in composition to sheeted dikes were observed in the upper part of the plagiogranite bodies. Plagiogranite consists of granular quartz, plagioclase with normal zoning, amphibole, biotite and a few clinopyroxene grains. Plagioclase and quartz intergrowths are characteristic. Epidote and chlorite occur as secondary minerals. The composition of the minerals from a plagiogranite sample is given in Table 3.

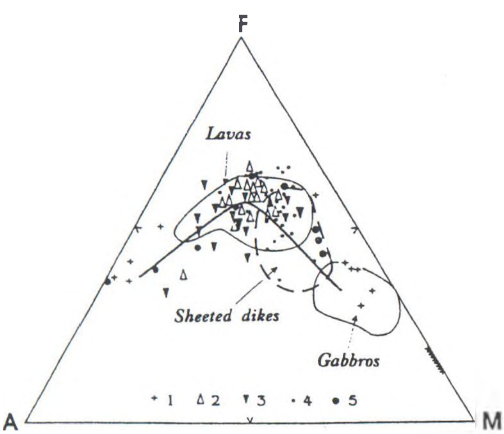

Fig. 4 - AFM diagram for the Kuyul ophiolitic rocks. 1-3 - Gankuvayam section: 1 - pillow lavas, 2 - dikes, 3 - peridotite, gabbro and plagiogranite; 4 - basalts beyond the Gankuvayam section. The line divides the tholeiitic and calc-alkali series (Irvine and Baragar, 1971).

Sheeted dike and pillow lava complex. A doleritic texture predominates in the dikes. Phenocrysts are andesine to labradorite, with minor pyroxene. The groundmass consists of plagioclase, augite, magnetite, and interstitial glass. Rocks with intersertal texture also occur (pyroxene dominates in microlithic mesostasis). There are also diabases containing quartz in phenocrysts. More felsic dikes corresponding in composition to andesite and diorite, contain quartz in the groundmass.

The extrusive portion of the section consists mainly of spherulitic lava sheets with massive, rarely finely-vesicular structure, in places with beds of unsorted globular hyaloclastite. Petrographically, the extrusive rocks are similar to the dike rocks. Phenocrysts consist of andesine and rarely labradorite; their amount increases sharply in the leucocratic varieties; augite predominates among dark-coloured phenocrysts. In andesites and dacites, quartz occurs among the phenocrysts, in the groundmass green hornblende and biotite predominate.

GEOCHEMISTRY

The major element composition and the contents of minor and trace elements in harzburgite, gabbro-troctolite-wehrlite and plagiogranite from the Gankuvayam ophiolitic section are reported in Table 1. Plotted in the AFM diagram (Fig. 4), the harzburgite shows a restite character, compared with harzburgite, the gabbro-wehrlite has lower XMg= Mg(100)/(Mg+Fe). Gabbros contain very low TiO_2.

Dikes and lavas have almost identical chemical composition, suggesting that they belong to the same magmatic suite. Both consist of a basalt-to-dacite (icelandite) differentiated series. Despite a high Na content in some samples, on the AFM diagram they fall into the field of the tholeiitic series. Basalt rocks of the Gankuvayam section differ from older basalts from the Kuyul ophiolites, which are believed to belong to mid oceanic ridges and seamounts. On the Ti-V diagram in fact, they plot in distinct fields (Fig. 5). The geochemical features of the basalts, particularly

Table 1 - Major (wt%) and trace (ppm) element analyses of harzburgites, wehrlites, troctolites, gabbros, plagiogranites, sheeted dikes and pillow lavas.

	1	2	3	4	5	6	7	8	9	10
Sample:	8x42-1	8x33-4	8x33-6	8x36-1	9p83-3	9p74-4	9p74-1	8x24-3	8x11	8x19-1
SiO2	38.65	38.05	49.40	39.41	42.65	46.60	73.98	55.69	49.42	60.30
TiO2	0.03	0.05	0.10	0.04	0.03	0.15	0.17	1.24	1.09	1.09
Al2O3	1.03	14.26	2.60	14.59	23.41	16.64	11.27	14.65	15.60	11.50
Fe2O3	4.55	1.51	0.80	3.21	0.51	1.88	1.41	5.91	9.17	5.67
FeO	3.75	1.90	4.70	3.77	1.79	4.56	1.96	4.85	3.45	3.54
MnO	0.13	0.07	0.11	0.10	0.05	0.14	0.03	0.15	0.17	0.21
MgO	38.65	10.92	22.40	20.85	7.88	10.70	1.65	5.87	4.53	4.04
CaO	0.56	25.94	15.70	7.03	17.70	14.40	2.63	3.45	8.06	3.01
Na2O	-	-	0.18	0.17	0.96	1.10	5.64	3.60	4.27	4.52
K2O	-	-	0.04	0.81	0.07	0.38	0.80	0.03	0.33	2.40
P2O5	0.04	0.05	0.04	0.06	0.04	0.07	0.05	0.30	0.15	0.13
Loss	12.23	6.62	4.01	9.41	4.73	2.61	0.70	3.93	3.26	3.25
Total	99.84	99.57	100.22	99.81	99.97	99.31	100.42	99.67	99.50	99.66
H2O-	0.22	0.20	0.14	0.36	0.15	0.08	0.13	0.20	0.26	1.02
Rb	-	11	4	2	10	10	2	-	10	-
Sr	32	52	15	100	970	169	60	112	179	57
Ba	11	18	28	62	21	20	98	18	25	125
Zr	12	19	29	11	25	10	200	109	69	34
Nb	-	-	-	-	-	-	5	1	-	-
Y	6	33	3	5	14	9	44	36	18	27
La	10	6	4	6	5	3	18	17	-	8
Ce	1	4	5	7	14	12	30	19	-	11
Nd	17	4	10	9	15	15	21	18	11	10
Ni	1210	212	290	285	208	154	45	28	23	37
Co	67	45	26	60	58	50	10	81	13	94
Cr	813	770	750	817	608	520	310	240	27	250
V	24	67	65	21	140	150	40	130	135	135
Cu	13	150	120	45	135	161	25	54	51	63

1 - Harzburgite, 2 - Gabbro, 3 - Wehrlite, 4 - Troctolite, 5 - OL-Gabbro-norite, 6 - Gabbro-norite, 7 - Plagiogranite, 8 - Andesite (Dike), 9 - Basalt (Lava), 10 - Andesite (Lava).

Table 2 - Major minerals and temperatures of crystallization of the ultramafic and mafic rocks from the Gankuvayam section

N	Sample	Rock Type	XMg			XMg	XCr	T, °C
			Ol	Opx	Cpx	Spinel		
1.	8x42-4	Harzburgite	90	91	91	57	45	1058
2.	8x42-2	-"-	90	91	93	54	51	1213
3.	8x42-1	-"-	91	92	92	59	53	1218
4.	8x47-1	-"-	89	90	92	41	73	977
5.	8x41-1	-"-	90	82	92	38	54	978
6.	8x41-1A	-"-	90	83	92	39	54	1023
7.	8x38-1	-"-	91	93	n.d.	56	58	
8.	8x37	-"-	91	92	n.d.	55	71	
9.	9P82-3	-"-	91	90	92	63	35	1010
10.	9P82-4	-"-	91	90	92	62	31	1004
11.	8x32-1	-"-	92	90	94	31	62	1216
12.	8x32-2	-"-	n.d.	80	n.d.	36	63	
13.	8x32-2A	-"-	92	81	n.d.	29	63	
14.	8x32-4	-"-	92	91	94	49	60	1375
15.	8x32-5	-"-	91	92	91	50	60	1204
16.	8x32-6	-"-	92	92	94	55	57	1172
17.	8x32-7	Harzburgite	92	92	93	67	32	1099
18.	9P75-6	-"-	91	90	92	64	37	1049
19.	9P75-7	-"-	92	90	89	63	44	1015
20.	9P75-8	-"-	91	92	92	64	28	1087
21.	8x33-1	-"-	95	93	n.d.	53	64	
22.	8x33-2	Dunite	92	92	90	50	65	1152
23.	8x33-4	Gabbro	75	86	91	49	60	1157
24.	8x33-5	-"-	n.d.	87	90	40	58	1120
25.	8x33-6	Wehrlite	87	94	87	30	58	1056
26.	8x33-6A	Wehrlite	n.d.	94	86	32	57	1111
27.	9P73-11	-"-	86	87	91	34	48	1026
28.	8x33-7	Gabbro	-	-	88	60	23	
29.	8x33-8	Gabbro-norite	-	90	n.d.	53	42	
30.	8x33-8A	-"-	90	91	n.d.	48	55	
31.	8x33-9	Gabbro	-	-	87	46	57	
32.	9P77-1	Wehrlite	93	95	95	40	57	1048
33.	9P77-3	Gabbro	89	92	95	61	48	1093
34.	8x4-1-8	-"-	94	81	90	41	40	1152
35.	8x4-1A	-"-	94	79	90	47	46	1059
36.	8x4-3	Wehrlite	n.d.	90	90	74	16	1221
37.	8x4-4	-"-	n.d.	90	92	62	38	1230
38.	8x4-6	-"-	91	82	90	28	57	1122
39.	8x4-9	Gabbro	89	90	89	78	8	995
40.	8x36-1	Troctolite	n.d.	90	91	47	51	1034
41.	8x36-2	-"-	86	85	88	n.d.	n.d.	1021
42.	9P82-1	Gabbro-norite	n.d.	79	89	36	40	834
43.	9P82-2	-"-	89	90	90	49	44	887
44.	9P82-6	-"-	77	75	75	8	65	947
45.	9P82-6A	-"-	77	72	76	62	31	766
46.	9P83-3	-"-	87	68	89	24	52	849
47.	9P83-6	-"-	88	69	79	33	42	978
48.	8x33-11	-"-	90	85	93	45	60	1156
49.	8x33-12	Gabbro	88	-	87	36	58	
50.	8x33-13	-"-	-	-	82	41	44	
51.	8x34-1	-"-	-	69	82	46	37	1016
52.	9P73-1	Gabbro-norite	-	90	91	64	30	886
53.	9P73-4	-"-	88	n.d.	88	74	24	
54.	9P73-3	Wehrlite	n.d.	92	92	69	28	1151
55.	9P73-5	-"-	92	93	94	73	34	1191
56.	9P73-7	-"-	n.d.	91	91	72	19	1046
57.	9P73-9	-"-	90	92	93	42	47	919
58.	9P73-10	Gabbro	85	-	89	26	37	
59.	9P73-10A	-"-	85	-	92	27	51	
60.	9P73-12	-"-	87	88	89	35	54	957
61.	9P73-13	Gabbro	-	-	87	38	46	
62.	9P73-15	Wehrlite	90	92	89	37	46	948
63.	9P72-6A-1	-"-	84	84	88	19	50	932
64.	9P72-6A-2	-"-	81	80	89	41	52	852
65.	8x34-4	Gabbro-norite	-	91	91	67	35	1194
66.	8x34-7	-"-	-	89	83	56	57	
67.	8x35	-"-	-	87	81	56	47	1066
68.	9P74-3	-"-	-	85	86	47	62	989
69.	9P74-4	-"-	-	84	87	34	58	1100
70.	9P83-8	Gabbro	-	-	72	47	70	

n.d. = not determined; XMg = Mg(100)/(Mg+Fe+Mn); XCr = Cr(100)/(Cr±Al). The temperature of crystallization was determined by two pyroxene geothermometer (4).

Table 3 - Representative chemical composition of constituent minerals in harzburgites, wehrlites, gabbros, plagiogranites sheeted dikes and pillow lavas of the Gankuvayam ophiolitic section

Sample:	Harzburgite,8x42-1				Gabbro,8x33-4				
Mineral	OL	Opx	Cpx	Sp	OL	Opx	Cpx	Sp	Pl
SiO2	38.35	54.43	52.98	-	39.74	54.15	54.20	-	44.95
TiO2	0.11	0.12	0.10	0.11	0.05	0.14	0.08	0.29	0.05
Al2O3	0.08	2.18	2.34	26.24	0.28	1.48	2.04	20.01	35.38
Cr2O3	0.14	0.86	0.95	44.60	0.34	0.48	0.56	45.42	-
FeO	9.15	5.96	2.51	15.96	14.74	9.21	2.87	22.66	0.12
MnO	0.17	0.15	0.11	0.14	0.16	0.32	0.14	0.18	0.10
MgO	52.79	35.49	17.15	12.69	45.11	32.77	16.86	11.95	-
CaO	0.10	1.05	22.76	-	0.01	2.04	23.41	-	18.73
Na2O	0.06	-	0.20	-	-	-	0.25	-	0.89
K2O	0.03	-	-	-	-	-	0.04	-	0.02
Total	100.98	100.90	99.10	99.74	100.43	100.59	100.45	99.91	100.16
O=	4	6	6	32	4	6	6	32	8
Si	0.936	1.925	1.942	-	1.131	1.903	1.961	-	2.213
Ti	0.002	0.004	0.003	0.020	0.001	0.004	0.002	0.055	0.002
Al	0.002	0.084	0.101	7.507	0.008	0.061	0.087	5.985	1.742
Cr	0.003	0.031	0.028	8.559	0.010	0.013	0.016	9.113	-
Fe+2	0.187	0.167	0.077	3.240	0.420	0.271	0.087	4.682	0.006
Mn	0.004	0.004	0.003	0.029	0.005	0.010	0.004	0.039	0.005
Mg	1.921	1.796	0.937	4.592	1.284	1.717	0.910	4.521	-
Ca	0.003	0.047	0.894	0.000	0.000	0.077	0.908	-	0.922
Na	0.003	-	0.014	-	-	-	0.018	-	0.044
K	0.001	-	-	-	-	-	0.002	-	0.001
Total	3.061	4.058	3.999	23.947	2.859	4.056	3.995	24.396	4.935
XMg,An	91.1	91.5	92.4	58.6	75.4	86.4	91.3	49.1	97.9
XCr		26.9	21.7	53.3		17.6	15.5	60.4	
Wo		2.3	46.9			3.7	47.7		
En		89.4	49.1			83.1	37.8		

Sample:	Wehrlite,8x33-6				Ol-Gabbro-norite,9p83-3				
Mineral	OL	Opx	Cpx	Sp	OL	Opx	Cpx	Sp	Pl
SiO2	39.57	56.06	53.26	-	40.78	53.96	52.10	-	48.93
TiO2	0.05	0.10	0.10	0.32	-	0.03	0.48	1.48	-
Al2O3	0.27	0.57	3.58	18.88	0.10	0.94	3.41	19.86	32.38
Cr2O3	0.34	0.45	0.98	38.74	0.06	-	1.02	31.78	-
FeO	12.16	4.57	3.60	33.05	12.24	20.17	3.29	39.68	0.72
MnO	0.16	0.18	0.27	0.40	0.20	0.37	0.12	0.47	-
MgO	48.01	38.52	14.43	8.10	45.70	23.78	16.40	6.98	-
CaO	0.02	0.10	23.83	-	0.03	1.14	22.47	-	15.59
Na2O	-	-	0.27	-	-	-	0.46	-	2.40
K2O	-	-	-	-	-	-	-	-	-
Total	100.56	100.55	100.24	100.49	99.11	100.39	99.75	100.25	100.02
O=	4	6	6	32	4	6	6	32	8
Si	0.979	1.924	1.954	-	1.024	1.980	1.902	-	2.240
Ti	0.001	0.003	0.003	0.064	-	0.001	0.013	0.291	-
Al	0.008	0.023	0.155	5.941	0.002	0.041	0.147	6.294	1.747
Cr	0.008	0.015	0.036	8.177	0.003	-	0.029	6.755	-
Fe+2	0.252	0.131	0.110	7.380	0.257	0.619	0.101	8.923	0.028
Mn	0.003	0.005	0.008	0.090	0.004	0.011	0.004	0.107	-
Mg	1.771	1.971	0.789	3.224	1.710	1.301	0.893	2.798	-
Ca	0.001	0.004	0.937	-	0.001	0.045	0.879	-	0.766
Na	-	-	0.019	-	-	-	0.033	-	0.207
K	-	-	-	-	-	-	-	-	-
Total	3.023	4.076	4.011	24.877	3.001	3.998	4.001	25.176	4.988
XMg,An	87.4	93.8	87.2	30.7	86.9	67.8	89.5	24.3	78.5
XCr		39.5	18.8	57.9	-	-	16.5	51.8	
Wo		0.2	51.0			2.3	46.9		
En		93.6	42.9			66.2	47.7		

Table 3 (continued)

Sample:	Gabbro-norite,9p74-4				Gabbro,9p83-8				
Mineral	Opx	Cpx	Sp	Pl	Cpx	Amph	Sp	Mt	Pl
SiO2	54.75	53.96	–	46.20	49.70	43.21	–	–	54.26
TiO2	0.20	0.16	0.39	0.11	2.70	1.35	0.95	16.40	–
Al2O3	2.10	2.33	19.70	34.10	4.30	14.40	11.98	2.10	30.20
Cr2O3	0.48	0.42	38.68	0.09	0.12	0.31	41.78	13.78	–
FeO	10.48	4.08	33.11	0.38	9.41	8.50	30.27	44.76	–
MnO	0.28	0.28	0.55	0.12	0.15	0.10	0.08	0.20	–
MgO	31.88	16.00	6.89	–	13.44	15.30	14.79	1.77	–
CaO	0.54	22.98	–	18.66	20.56	11.61	–	–	10.35
Na2O	–	0.18	–	1.09	0.44	3.05	–	–	4.40
K2O	–	–	–	–	–	0.30	–	–	0.15
Total	100.71	100.39	99.32	100.75	100.82	98.13	99.85	102.63	99.36
O=	6	6	32	8	6	23	32	32	8
Si	1.907	1.963	–	2.119	1.844	6.217	–	–	2.608
Ti	0.005	0.004	0.078	0.004	0.075	0.146	0.191	3.536	–
Al	0.186	0.100	6.207	1.844	0.188	2.442	3.778	0.710	1.452
Cr	0.013	0.009	8.174	0.001	0.004	0.035	8.838	3.124	–
Fe+2	0.305	0.124	7.402	0.015	0.292	1.023	6.774	10.731	–
Mn	0.008	0.009	0.125	0.005	0.005	0.012	0.017	0.040	–
Mg	1.655	0.868	2.746	–	0.743	3.282	5.900	0.757	–
Ca	0.020	0.896	–	0.917	0.817	1.790	–	–	0.497
Na	–	0.011	–	0.097	0.032	0.851	–	–	0.211
K	–	–	–	–	–	0.551	–	–	0.007
Total	4.099	3.984	24.731	5.002	4.000	15.851	25.501	24.000	4.775
XMg,An	84.4	87.4	27.1	89.9	71.8	76.2	46.6	66.0	69.51
XCr	–	–	56.8		–	–	70.1	81.5	
Wo	1.0	47.5			44.1			–	
En	83.6	45.9			40.1			–	

Sample:	Plagiogranite,9p74-1				Dolerite (Dike),9p72-1		
Mineral	Hb	Bi	Pl	Mt	Cpx	Amph	Pl
SiO2	44.88	38.97	62.31	–	50.96	50.12	51.16
TiO2	0.72	2.11	–	48.13	0.82	0.44	–
Al2O3	10.70	16.76	24.59	–	3.50	4.16	30.64
Cr2O3	0.54	0.03	–	3.05	0.40	0.11	–
FeO	16.47	10.48	0.26	45.89	10.50	17.86	0.07
MnO	0.04	0.03	–	2.54	0.23	0.21	–
MgO	12.78	16.71	–	0.05	13.79	11.64	–
CaO	10.16	–	5.68	0.19	19.82	12.40	13.51
Na2O	1.98	0.28	7.85	–	0.31	0.87	3.89
K2O	0.64	9.97	0.24	–	–	0.10	0.11
Total	98.91	95.34	100.93	99.85	100.33	97.91	99.38
O=	23	22	8	32	6	23	8
Si	6.597	5.674	2.737	–	1.900	7.435	2.341
Ti	0.080	0.231	–	9.916	0.023	0.049	–
Al	1.854	2.876	1.273	–	0.154	0.727	1.652
Cr	0.063	0.004	–	0.661	0.012	0.013	–
Fe+2	2.025	1.276	0.009	10.513	0.327	2.216	0.027
Mn	0.005	0.004	–	0.589	0.007	0.026	–
Mg	2.800	3.627	–	0.020	0.767	2.574	–
Ca	1.600	–	0.267	0.056	0.792	1.971	0.662
Na	0.564	0.079	0.668	–	0.022	0.250	0.345
K	0.120	1.852	0.013	–	–	0.019	0.006
Total	15.708	15.623	4.967	21.755	4.005	15.280	5.033
XMg,An	58.0	74.0	28.2	–	70.1	54.4	65.3
XCr	3.3	0.1		–	–	–	
Wo				–	42.0		
En				–	40.7		

Table 3 (continued)

Sample:	Andesite(Dike),8x24-3			Basalt(Lava),8x11		
Mineral	Cpx	Amph	Pl	Cpx	Amph	Pl
SiO2	50.05	45.97	55.22	51.55	49.18	56.24
TiO2	0.65	1.09	-	0.74	1.52	-
Al2O3	4.93	14.68	28.04	4.60	5.18	28.60
Cr2O3	0.02	0.21	-	0.02	-	-
FeO	10.59	7.22	0.16	12.01	19.39	0.27
MnO	0.27	0.20	0.02	0.32	0.47	-
MgO	13.97	11.00	0.07	15.17	10.72	-
CaO	18.97	15.73	10.80	17.68	12.60	9.68
Na2O	0.05	0.73	4.83	0.04	0.54	5.48
K2O	0.02	0.32	0.18	0.03	0.03	0.23
Total	99.52	97.18	99.34	100.16	99.64	100.50
O=	6	23	8	6	23	8
Si	1.876	6.602	2.501	1.883	7.230	2.512
Ti	0.018	0.118	-	0.020	0.168	-
Al	0.218	2.485	1.497	0.198	0.898	1.506
Cr	0.001	0.024	-	0.001	-	-
Fe+2	0.332	0.867	0.006	0.367	2.384	0.010
Mn	0.009	0.024	0.001	0.010	0.059	-
Mg	0.780	2.355	0.005	0.826	2.350	-
Ca	0.762	2.420	0.524	0.692	1.985	0.463
Na	0.004	0.203	0.424	0.003	0.154	0.475
K	0.001	0.059	0.010	0.001	0.006	0.013
Total	4.001	15.157	4.968	4.001	15.234	4.979
XMg,An	70.1	73.1	54.7	69.2	49.6	48.7
XCr	-	-	-	-	-	-
Wo	40.7			36.7		
En	41.6			43.8		

Sample:	Andesite (Lava),8x19-1				
Mineral	Cpx	Amph	Sp	Pl	Mt
SiO2	50.76	47.15	-	55.48	-
TiO2	0.40	0.68	0.84	-	49.20
Al2O3	2.58	10.15	29.76	28.70	-
Cr2O3	0.03	0.05	29.58	-	0.28
FeO	10.97	18.87	26.11	0.25	47.78
MnO	0.41	0.28	0.21	0.01	1.16
MgO	13.87	7.56	13.20	-	1.05
CaO	20.88	12.16	-	10.75	-
Na2O	0.28	0.87	-	5.40	-
K2O	0.11	0.40	-	0.28	-
Total	100.29	98.17	99.70	100.87	99.47
O=	6	23	32	8	32
Si	1.901	7.008	-	2.482	-
Ti	0.011	0.076	0.155	-	10.134
Al	0.114	1.778	8.591	1.513	-
Cr	0.001	0.006	5.728	-	0.061
Fe+2	0.345	2.346	5.349	0.009	10.944
Mn	0.013	0.035	0.044	-	0.269
Mg	0.777	1.675	4.820	-	0.429
Ca	0.841	1.937	-	0.515	-
Na	0.020	0.251	-	0.468	-
K	0.005	0.076	-	0.016	-
Total	4.036	15.188	24.686	5.003	21.836
XMg,An	69.3	41.7	47.4	51.6	-
XCr	-	-	40.0	-	-
Wo	42.8				-
En	39.6				-

low Mg, Cr, and K, and the presence of intermediate and felsic rocks with low XMg suggest that the dike-extrusive complex of the Gankuvayam section in total has a tholeiitic serial character. The available data do not allow to discriminate between oceanic (Galapagos spreading center) and suprasubduction settings.

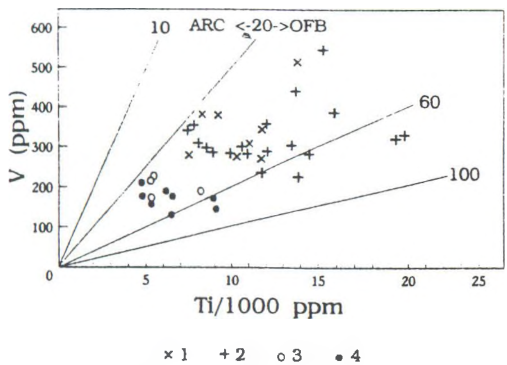

Fig. 5 - Two types of basaltic rocks of the Kuyul terrane on the Ti-V diagram (Shervais, 1982. 1-2 - Triassic-Early Jurassic basalts beyond the Gankuvayam section: 1 - to the north; and 2 - to the south; 3-4 - Late Jurassic Gankuvayam section: 3 - dikes, 4 - pillow-lavas.

MINERAL CHEMISTRY

The chemical composition of minerals in 80 samples of harzburgite, gabbro-wehrlite plagiogranite, sheeted dikes and pillow-lavas from the Gankuvayam section was studied using JXA-5A and Camebax microprobes in the Far East Geological Institute and Institute of Volcanology of the Far Eastern Branch, Acad. Sci. Russia. A brief description of the main rock-forming minerals of the Gankuvayam cross-section is given in Table 2 and the microprobe analyses of minerals are shown in Table 3.

In all cases, the compositions of primary minerals are typical of those reported in residual mantle peridotite and cumulus ultramafic and gabbroic rocks of well-known ophiolite complexes (Coleman, 1977; Himmelberg and Loney, 1980; Pallister and Hopson, 1981; Loney and Himmelberg, 1984).

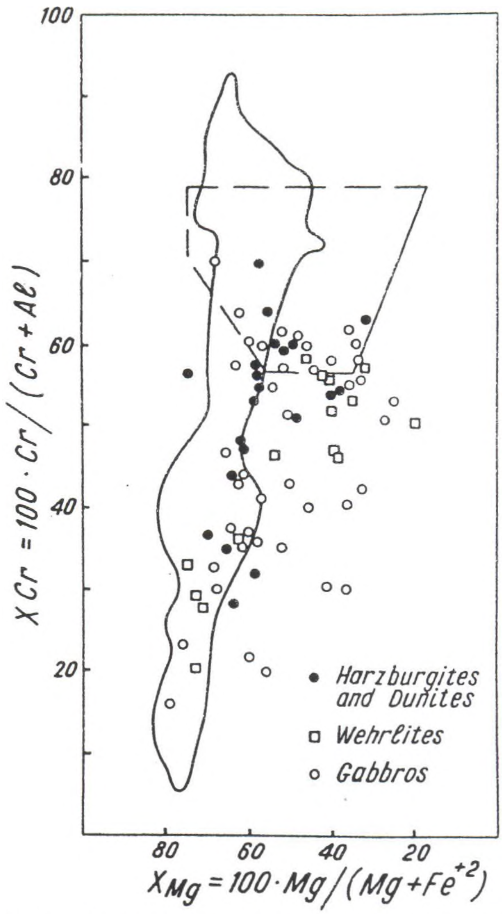

Fig. 6 - Composition of spinels from harzburgite and gabbro-wehrlite complexes.
Solid line - field of chrome-spinels of alpine-type peridotites. Dotted line - field of layered intrusives (Dick and Bullen, 1984).

Spinel. Chrome-aluminium spinel was analysed in harzburgites, gabbros and lavas. Spinel composition differs from that of alpine-type harzburgites in the lower Mg content

(Fig. 6). On the Cr-Al-Fe^{+3} diagram, spinel compositions are aligned along the Cr-Al side corresponding to a regular increase of Al content from the center towards the grain edge (Fig. 7). Relic spinel in gabbros is similar in composition to that of harzburgites, but aluminous spinel also occurs (Fig. 7). Chromian spinel in andesite (Table 3) is analogous in composition to that of tholeiitic ocean basalts (Dick and Bullen, 1984).

Olivine. Individual crystals are homogeneous. High XMg is typical of ultramafic and mafic rocks; though olivine has nearly the same XMg in harzburgite (90-92%), it varies from 94 to 77% in the gabbro-wehrlite portion (Table 2). There is a direct relationship between XMg in coexisting olivine and chromian spinel; the presence of orthopyroxene in the assemblage presumably does not control the composition of chromian spinel.

Orthopyroxene and clinopyroxene. Throughout the Gankuvayam section, XMg of these minerals is in good agreement with the composition of coexisting olivine. The composition of ortho- and clinopyroxene is that common of ophiolite rocks. In the uppermost part of the section, titanium clinopyroxene in assemblage with chromium titanomagnetite appears in massive medium-grained gabbro (Table 3). Calculated crystallization temperatures using two-pyroxene geothermometers (Wood and Banno, 1973; Wells, 1977) are similar: 977-1375°C for harzburgite, 1056-1230°C for wehrlite, and 918-1196°C for gabbro (Table 2).

In dike and lava complexes, orthopyroxene is absent and clinopyroxene has a lower Mg content compared to that in gabbro. Clinopyroxene compositions of the gabbroic and volcanic rocks plotted on the discriminant diagrams of Leterrier et al. (1982) (not shown) indicate that the pyroxenes crystallized from a tholeiitic magma.

Amphibole. Secondary amphibole produced by oceanic metamorphism characterizes the gabbro. It contains very low TiO_2 (0,10%). Only in the uppermost massive gabbros does magmatic pargasite appear in association with titanium-augite (see sample 9p83-8 in Table 3).

Plagioclase. It is represented by calcic varieties containing 70% to 90% anorthite. Grains are homogeneous, indicating a slow cooling rate sufficient for chemical equilibrium.

DISCUSSION

The Late Jurassic differentiated volcanic rocks of the Gankuvayam section differ sharply from the typical oceanic basalts of the Triassic and Early Jurassic Kuyul ophiolites. Consequently, we infer that the Gankuvayam section may represent a secondary spreading center in the oceanic basin. Geochemical data suggest that the Gankuvayam pillow-lavas are comparable with the tholeiitic lavas of a supra-subduction zone. Geological data indicate that the Gankuvayam spreading center developed and accreted transversely to the Early Cretaceous active margin as the Galapagos type spreading center (Khanchuk et al., 1990).

The mineral chemistry presented in this work shows regular and gradual changes upward in the Gankuvayam ophiolitic section, closely related with the rock chemistry, which indicates an unique petrologic assemblage. High-Mg harzburgites, gabbro and wehrlites are associated with low-Mg sheeted dikes and pillow-lavas. Olivine and pyroxenes of harzburgites, gabbro and wehrlites have consistently high Mg content, and the chromian spinel have low Mg content.

The lower part of the gabbro-wehrlite unit may be the basal cumulates representing a solidified magma chamber at the crust-mantle boundary of the paleospreading zone. The higher levels of gabbro and plagiogranite appear to occur as simultaneous intrusions. The harzburgite is considered to represent the residuum of partial melting and extraction of a basaltic magma. The texture, the limited or absent mineral compositional range, and the general absence of mineral compositional zoning indicate that the layered gabbros are adcumulates.

Dick and Bullen (1984) have proposed to use the composition of chromian spinel in peridotite as a petrogenetic indicator of the tectonic environment. They clearly indicated that the XCr of chromian spinel increases as the degree of depletion increases, and they proposed that many ophiolites have a complex multistage origin involving oceanic crust and supra-subduction environments.

The full range of chromian spinel compositional data for the Gankuvayam ophiolite is typical of peridotites that Dick and Bullen (1984) interpret as having complex multistage melting histories, involving the development of spreading centers on oceanic crust in supra-subduction zones or ocean margins.

We conclude that among the ophiolitic sections known in Eastern Asia, the Gankuvayam one represents a complete ophiolite with well-preserved magmatic mineral assemblages and could be recommended as a type study area to investigate ophiolite formation processes.

Acknowledgements

The research described in this publication was made possible, in part, by Grant N RY 1000 from the International Science Foundation.

REFERENCES

Alekseev S.E., 1981. Kuyul serpentinitic melange and structure of the Talovsko-Mainskoi zone (Koryak upland). Geotectonica, 1: 105-120 (in Russian).

Chekhov A.D., 1982. Tectonics of the Talovsko-Pekulneiskoi zone. In: Essais on the tectonics of the Koryak upland. Nauka, Moscow, p. 10-106 (in Russian).

Coleman R.G., 1977. Ophiolites. Springer-Verlag, New York, 229 p.

Dick H.J.B. and Bullen T., 1984. Chromian spinel as a petrogenetic indicator in abyssal and alpine-type peridotites and spatially associated lavas. Contrib. Mineral. Petrol., 86: 54-76.

Himmelberg G.R. and Loney R.A., 1980. Petrology of ultramafic and gabbroic rocks of the Canyon Mountain ophiolite, Oregon. Am. J. Sci., 280-A: 232-268.

Irvine T.N. and Baragar W.R.A., 1971. A guide to the chemical classification of the common volcanic rocks. Canad. J. Sci., 8: 523-548.

Khanchuk A.I., Grigoryev V.N., Golozubov V.V., Govorov G.I., Krylov K.A., Kurnosov V.B., Panchenko I.V., Pralnikova I.E. and Chudaev O.V., 1990. The Kuyul ophiolite terrane, Vladivostok, Far Eastern Branch of the USSR Acad. Sci., 108 p. (in Russian).

Leterrier J., Mauky R.C., Thonon P.G., Girard G. and Marchal M., 1982. Clinopyroxene composition as method of identification of the magmatic affinities of paleovolcanic series. Earth Planet. Sci. Lett., 59: 139-154.

Loney R.A. and Himmelberg G.R., 1989. The Kanuti Ophiolite, Alaska. J. Geoph. Res., 94 (B11): 15869-15900.

Pallister J.S., and Hopson C.A., 1981. Samail ophiolite plutonic suite: Field relations, phase variation, cryptic variation and layering and a mode of spreding ridge magma chamber. J. Geoph. Res., 86: 2593-2644.

Shervais J.W., 1982. Ti-V plots and the petrogenesis of modern and ophiolitic lavas. Earth Planet. Sci. Lett., 59: 101-118.

Wells P.R.A., 1977. Pyroxene thermometry in simple and complex systems. Contrib. Mineral. Petrol., 62: 129-139.

Wood B. and Banno S., 1973. Garnet-orthopyroxene and orthopyroxene-clinopyroxene relationships in simple and complex systems. Contrib. Mineral. Petrol., 42: 109-124.

Received, January 11, 1992
Accepted, September 20, 1994